

Landau quantization and the Aharonov-Bohm effect in a two-dimensional ring

W.-C. Tan and J. C. Inkson

Department of Physics, University of Exeter, Exeter, EX4 4QL, United Kingdom

(Received 3 March 1995; revised manuscript received 28 September 1995)

We propose an exactly soluble model for a ring with finite width. Exact energy spectra and wave functions are obtained analytically for a ring in the presence of both a uniform perpendicular magnetic field and a thin magnetic flux through the ring center. We use the model to study the Aharonov-Bohm (AB) effect in an ideal annular ring that is weakly coupled to both the emitter and the collector. It is found that, for such a weakly coupled ring in a uniform magnetic field, not only do the electron states in *different* subbands of the ring produce different AB frequencies, the clockwise and anticlockwise moving states in the *same* subband also lead to two different AB frequencies. Therefore, when many subbands in the ring are populated, the large number of different AB frequencies generally result in an aperiodic AB oscillation. More striking is that, even when only *one* subband is populated, the two AB frequencies corresponding to the states moving in opposite directions also cause beating in the AB oscillations. We have obtained explicit expressions for all these AB frequencies. Our results produce a clear explanation for the recent experimental observation of Liu and co-workers.

Recently, the electronic properties of low-dimensional structures with a ring geometry have been extensively studied including Aharonov-Bohm (AB) effects,¹⁻⁹ persistent currents,¹²⁻²⁰ and quantum chaos.¹³ The original picture of both the AB effect and the persistent current in a ring geometry is very simple: Considering a one-dimensional (1D) ring pierced by an AB magnetic flux (i.e., an infinitely thin flux tube) confined to its center, the magnetic flux has a purely gauge effect. As a consequence of gauge invariance, the electron eigenenergies of the ring are periodic in the magnetic flux with period $\phi_0 = h/e$. If the ring is connected to an emitter and a collector, this will lead to a periodic oscillation in the conductance, the so-called AB oscillations. In the case of an isolated ring in thermal equilibrium, there will be a *persistent* charge current that also oscillates with the magnetic flux.¹¹

Experimental studies on the AB effect and persistent currents in ringlike devices have continuously revealed interesting phenomena that cannot be explained by a simple theory. For example, in the early experimental study of the AB effect in small metal rings¹ it was found that the amplitudes of the AB oscillation in conductance were usually dominated by random fluctuations of the order of e^2/h . This led to the discovery of the universal conductance fluctuations.¹⁰ In the case of persistent currents, the unpredicted large amplitude of the measured current in metal rings¹⁴ has led to important questions that still attract considerable interest.

One of the most important factors that cause complications in real experiments is the finite width of the rings. In a ring with a finite width, *not only are multiple channel effects important, the penetration of the uniform magnetic field, which is used in all practical experiments, into the conducting region of a ring also plays an important role.* Significant theoretical efforts have been devoted to the study of the finite-width effect on AB oscillations⁶⁻⁸ and persistent currents.¹⁶⁻²⁰ However, because of the difficulty in dealing with the 2D annular geometry, in most theoretical work rings with a finite width are approximated by more manageable

models, such as 2D or 3D *straight wires* with periodic boundary conditions^{17,18} or a 2D cylinder.²⁰

Theoretical studies on the electron states in a real annular geometry have been mainly based on semiclassical approaches. A qualitative analysis of the electronic states was performed by Halperin²¹ to clarify the physical picture of the quantum Hall effect, and by Jain⁷ in the study of the AB effect in the quantum Hall regime. The semiclassical approach has also been used by Beenakker, Houten, and Staring⁸ to calculate the magnetic-field dependence of the energy levels, and by Groshev, Kostadinov, and Dobrianov¹⁹ to calculate the persistent current. Recently, full quantum-mechanical calculations based on numerically solving the Schrödinger equation for a 2D ring in a uniform magnetic field have also been used in the study of persistent currents.¹⁶ However, in a semiconductor ring used in actual experiments,^{3,15} the number of electrons is typically 10^3 or bigger (the number is much larger in a metallic ring^{1,14}). The knowledge of the energies and wave functions of all the electrons as well as their magnetic-field dependence is essential for a complete description of the AB effects or persistent currents in a ring. Therefore it requires extensive computational power to solve the Schrödinger equation numerically for a 2D ring. This strongly limits the flexibility of the numerical approach.

In this paper, we propose a simple model potential that describes an isolated ring with finite width. The model is very flexible; both the radius and the width of the ring can be adjusted independently by suitably choosing the two model parameters. In particular limits it can also describe a quantum dot, an antidot, a 1D ring, and a straight 2D wire. Exact energy spectra and wave functions are obtained analytically in this model with a uniform magnetic field applied perpendicular to the ring and a magnetic flux confined to its center. Our model, therefore, provides a convenient theoretical tool for studying electron states and their magnetic-field dependence in an ideal 2D ring, and allows a direct comparison between the electronic states in a 2D ring and those in other geometries, such as a dot, an antidot, a 1D ring, and a

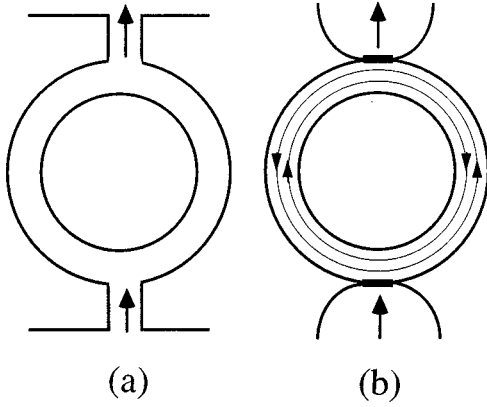


FIG. 1. (a) Schematic illustration of the single ring device used in Ref. 3; (b) the weakly coupled ring model used in our calculations.

straight 2D wire. The exact solutions of the model can be used to examine the accuracy of the results obtained from numerical calculations or other approximations. It also provides a firm starting point for the investigation of more complicated situations, such as disorder effects and electron-electron interaction.

As an illustration and application of our model, we have studied the effects of finite width on the AB oscillations in an ideal 2D ring to model the recent experimental results of Liu *et al.*³ on the correlation between AB effects and the one-dimensional subband population in GaAs/Al_xGa_{1-x}As rings. The geometry of the ring used in Ref. 3 is schematically shown in Fig. 1(a). Liu and co-workers³ found that, when four spin-degenerate subbands in the ring are populated, the AB interference patterns are dominated by random features. When only one subband is occupied in the ring, well-defined periodic AB oscillation together with an amplitude beating effect occurs. They suggested that this random feature is due to both the penetration of magnetic field into the conducting region of the ring and disorder scattering, but the exact reasons for the change of the AB patterns from a random state to an ordered one and the origin of amplitude beating in the case of one occupied subband were not identified.

In our model the 2D ring is defined in the X - Y plane by a radial potential of the form

$$V(r) = a_1 r^{-2} + a_2 r^2 - V_0, \quad (1)$$

where $V_0 = 2\sqrt{a_1 a_2}$. The potential has a minimum $V(r_0) = 0$ at $r_0 = (a_1/a_2)^{1/4}$, so r_0 defines the averaging radius of the ring. For r near r_0 , the potential of the ring has the simple parabolic form $V(r) \cong \frac{1}{2}\mu\omega_0^2(r-r_0)^2$, where $\omega_0 = \sqrt{8a_2/\mu}$ and μ is the electron effective mass in the semiconductor. A useful definition of the effective width of the ring at a given Fermi energy E_F is then $\Delta r = \sqrt{8E_F/\mu\omega_0^2}$.

Both the radius and the width of the ring can be adjusted independently by suitably choosing a_1 and a_2 . The model can also be used to describe several different physical systems: a one-dimensional ring for $r_0 = \text{constant}$ and $\omega_0 \rightarrow \infty$, a straight 2D wire for $\omega_0 = \text{constant}$ and $r_0 \rightarrow \infty$, a single quantum dot for $a_1 = 0$ (see also Ref. 23) and an isolated antidot for $a_2 = 0$.

In the presence of a uniform magnetic field B perpendicular to the X - Y plane, the Hamiltonian of an electron is

$$H = \frac{\hbar^2}{2\mu} \left[-\frac{1}{r} \frac{\partial}{\partial r} \left(r \frac{\partial}{\partial r} \right) - \frac{1}{r^2} \frac{\partial^2}{\partial \varphi^2} - i \frac{eB}{\hbar} \frac{\partial}{\partial \varphi} + \frac{e^2 B^2}{4\hbar^2} r^2 \right] + \frac{a_1}{r^2} + a_2 r^2 - V_0, \quad (2)$$

where the vector potential is chosen as $\mathbf{A} = \frac{1}{2}Br\hat{\varphi}$ and we ignore the spin of the electron.

It can be easily shown that the eigenvalues and eigen wave functions of the Hamiltonian are

$$E_{n,m} = \left(n + \frac{1}{2} + \frac{M}{2} \right) \hbar\omega - \frac{m}{2} \hbar\omega_c - \frac{\mu}{4} \omega_0^2 r_0^2, \quad n = 0, 1, 2, \dots, \quad m = \dots, -1, 0, 1, \dots, \quad (3)$$

$$\Psi_{n,m}(r, \varphi) = \frac{1}{\lambda} \left(\frac{\Gamma(n+M+1)}{2^{M+1} n! [\Gamma(M+1)]^2 \pi} \right)^{1/2} \times e^{-im\varphi} e^{-(1/4)(r/\lambda)^2} \left(\frac{r}{\lambda} \right)^M \times {}_1F_1[-n, M+1, \frac{1}{2}(r/\lambda)^2], \quad (4)$$

where

$$\omega_c = \frac{eB}{\mu}, \quad \omega = \sqrt{\omega_c^2 + \omega_0^2}, \quad \lambda = \sqrt{\frac{\hbar}{\mu\omega}}, \quad M = \sqrt{m^2 + \frac{2a_1\mu}{\hbar^2}}, \quad (5)$$

and ${}_1F_1$ is the confluent hypergeometric function. The quantum numbers n and m characterize the radial motion and the angular momentum, respectively. In relation to a circular wire, n can be viewed as the subband index, and m the quantum number describing the longitudinal motion in the wire.

From the above solutions, we can see that the electron states in the 2D ring have the following properties.

(a) *The subband dispersions of a 2D ring are strongly nonparabolic* even if $B=0$, which is in strong contrast to the case of a 1D ring or a 2D straight wire.²⁴ Such nonparabolicity is essentially due to the existence of the centrifugal potential in a 2D ring, which makes different states in the same subband having different radial wave functions, and therefore the subband dispersions depend on the actual radial confinement potential.

(b) At $B=0$, the minima of all subbands are at $m=0$ and the subband dispersions are symmetric about $m=0$. When $B \neq 0$, the subband dispersions are no longer symmetric about the subband minima and the bottoms of all the subbands are shifted to a nonzero quantum number $m_0 = eBr_0^2/2\hbar$, which is exactly the number of quantum flux circles by a ring with a radius r_0 .

(c) The radius $r_{n,m}$ and the width $d_{n,m}$ of a ring state (n, m) can be expressed as²²

$$r_{n,m} = (2M)^{1/2} \lambda \quad \text{and} \quad d_{n,m} = 2(2n+1)^{1/2} \lambda, \quad (6)$$

respectively. At $B=0$, the $m=0$ states have the smallest radius, which is equal to the average ring radius r_0 , and therefore *all the other states are centered in the outer side half of the conducting region of the 2D ring*. One can also verify²² that the radius of a state at the bottom of a subband ($m=m_0$) is always equal to the average radius of the ring, i.e., r_{m_0}

$\equiv r_0$. Because all states with $|m| < m_0$ have radii smaller than r_0 , increasing the magnetic field will push more and more states into the inner side of the ring.

(d) If, in addition to the uniform magnetic field, there is also an AB flux $\Phi = \ell \phi_0$ penetrating through the center of the 2D ring, the energy spectra and wave functions can then be obtained by a gauge transformation of the results given in Eqs. (3)–(5), resulting in a change of m to $m - \ell$.²²

We now consider a 2D ring that is coupled to two leads, as shown in Fig. 1. The conductance of the system is given by the Landauer-Büttiker formula,⁶

$$G(B) = \frac{2e^2}{h} \sum_n T_n(B, E_F), \quad (7)$$

where $T_n(B, E_F)$ is the magnetic-field-dependent transmission coefficient of the n th channel in the leads at the Fermi energy E_F . The factor of 2 comes from the spin degeneracy. If we assume that the two leads are weakly coupled to the ring, as shown in Fig. 1(b), the electron in one lead can reach the other one only by tunneling through the quasibound circular states in the ring. In such a case, the conductance can be approximately expressed in the form of²⁵

$$G(B) = \frac{2e^2}{h} \sum_{n,m} \frac{\Gamma_{n,m}^e \Gamma_{n,m}^c}{[E_F - E_{n,m}(B)]^2 + (\Gamma_{n,m}^e + \Gamma_{n,m}^c + \Gamma_{n,m}^i)^2/4} \times \frac{\Gamma_{n,m}^e + \Gamma_{n,m}^c + \Gamma_{n,m}^i}{\Gamma_{n,m}^e + \Gamma_{n,m}^c}. \quad (8)$$

$E_{n,m}(B)$ is the energy of the (n, m) th quasibound ring states. Furthermore, we can approximate the energies of these quasibound states with those of the isolated ring given in Eq. (3). $\Gamma_{n,m}^e$ ($\Gamma_{n,m}^c$) and $\Gamma_{n,m}^i$ are the broadening of the (n, m) th ring state caused by leaking into the emitter (collector) and inelastic scattering, respectively. The elastic broadening is determined by the overlap between the bound ring state and the extended states in the leads, which can be evaluated using the wave functions given in Eq. (4). Since we are here interested in the weak-field ($\omega_c \ll \omega_0$) AB effect, the electron states in the ring are dominated by the confinement potential of the ring. For simplicity, we ignore the magnetic-field dependence and the quantum-number dependence of the elastic broadening.

To mimic the GaAs/Al_xGa_{1-x}As ring used in the experiment of Ref. 3, we set $a_1 = 9.1022 \times 10^6$ meV nm² and $a_2 = 2.222 \times 10^{-5}$ meV nm⁻², which gives a ring radius $r_0 = 800$ nm and a ring width $\Delta r = 300$ nm at $E_F = 2$ meV. The electron effective mass is taken to be $\mu = 0.067 m_e$. By changing the Fermi energy E_F we can adjust the subband population. In the calculation, we take $\Gamma_{n,m}^i = \Gamma^i = 0.004$ meV corresponding to the thermal broadening at the experimental temperature³ $T \approx 40$ mK. The elastic broadening is taken to be $\Gamma_{n,m}^e = \Gamma_{n,m}^c = \Gamma^{\text{el}}/2 = 0.005$ meV.

Figure 2 shows the calculated resistance ($R = G^{-1}$) as a function of magnetic field. Curves (a) and (b) in Fig. 2 are calculated with one ($E_F = 0.5$ meV) and four ($E_F = 2.0$ meV) populated spin degenerate subbands, respectively. The beating and the increasing apparent random nature of the oscillation amplitude seen in experiment³ are clearly reproduced. Since the AB oscillation directly reflects the oscillation of the density of states of the 2D ring at the Fermi energy, the result

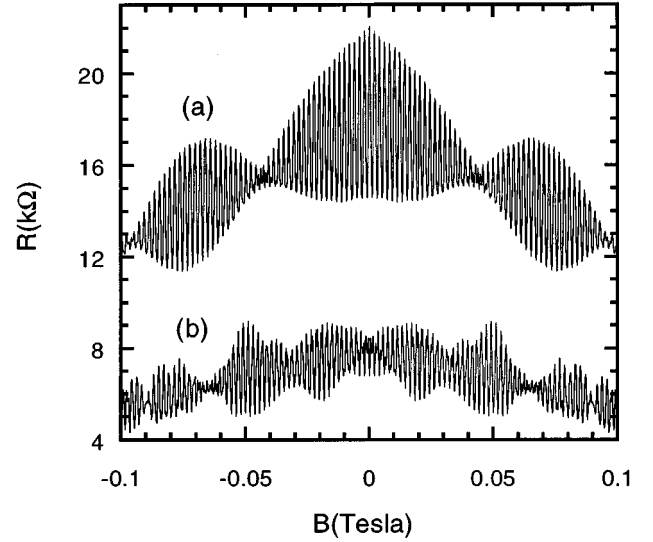


FIG. 2. Magnetoresistances for two different subband populations in a 2D ring. (a) $E_F = 0.5$ meV, (b) $E_F = 2.0$ meV. See text for details.

shown in Fig. 2 can be understood by looking at the magnetic-field dependence of the eigenenergies of the 2D ring shown in Fig. 3. It can be seen that, with increasing magnetic-field strength, the energy of a ring state (n, m) is shifted upward or downward depending on the direction of the electron motion. The sweeping of the electronic states in each subband through the Fermi energy with varying the magnetic field strength will lead to two sets of oscillations

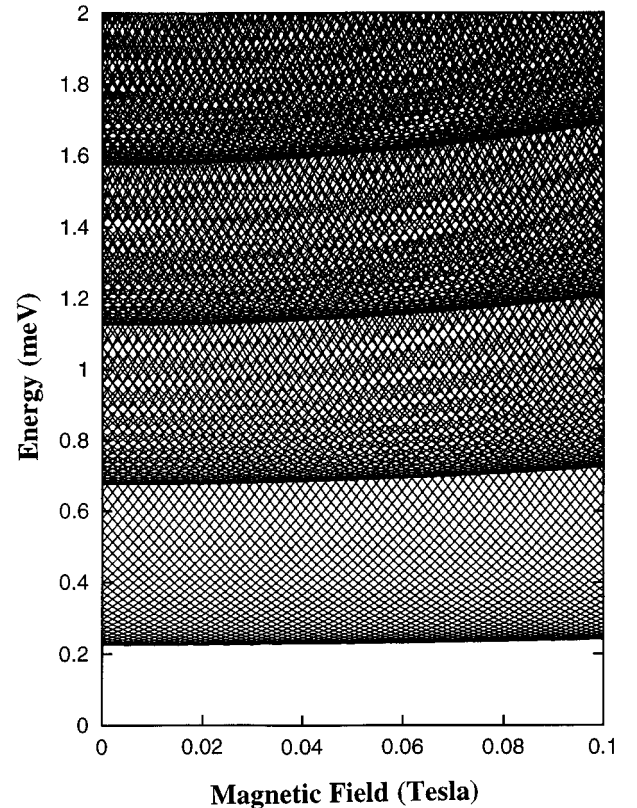


FIG. 3. The energy levels in a 2D ring as a function of magnetic-field strength.

in the magnetoresistance, corresponding to the clockwise and anticlockwise moving states, respectively.

Figure 3 shows clearly that different oscillations have different frequencies. Hence in the case when four spin degenerate subbands are populated, the superposition of the eight sets of oscillations of different periods results in an apparent aperiodic oscillation as shown in curve (b) of Fig. 2. Even when only one spin degenerate subband is occupied, the beating of the two sets of oscillations corresponding to the states moving in the opposite directions leads to a modulation of the AB oscillation amplitudes as shown in curve (a) of Fig. 2. It is interesting to point out that the beating effect shown in curve (a) is beyond the description of the well-developed theory for AB effects in 1D rings,^{6,7} reflecting the importance of the geometry.

In our model, each AB frequency can be exactly expressed as²²

$$f_{n,m} = \frac{\partial m}{\partial B} \Big|_{E_F} = \frac{\pi r_{n,m}^2}{\phi_0} \left[1 - \frac{(2n+1)\omega_c}{m\omega - M\omega_c} \right], \quad (9)$$

where $r_{n,m}$ is the radius of the (n,m) th state, which is passing through the Fermi energy. Equation (9) shows that the AB frequency of a given set of oscillation depends on not only the radii of the ring states but also the magnetic-field strength and the ring parameters. Such a complexity has not been noted previously. Only in the weak magnetic-field limit ($\omega_c \ll \omega_0$) and away from the subband depopulation regions does Eq. (9) reduce to the familiar form $f_{n,m} = \pi r_{n,m}^2 / \phi_0$.

Since the ring parameters used in our calculation are very similar to those of the device used in the experiment,³ we can compare our calculated magnetoresistance in Fig. 2 with the experimental results shown in Fig. 2 of Ref. 3 directly. It can be seen that our calculated magnetoresistances have reproduced the main features of the experimental results, such as the correlation between the AB patterns and subband populations. Both the fundamental AB frequency and the period

of beating shown in Fig. 2 are in excellent agreement with the experimental results. In addition to the AB oscillations, both curves (a) and (b) of Fig. 2 show strong mean negative magnetoresistance. This is also observed in the experiment.³ The negative resistance in our calculation is due to the increasing of density of states at the Fermi energy with increasing magnetic field, as shown in Fig. 3. In view of the simplicity of our model, the agreement between theory and experiment is remarkable, and strongly suggests that the main features of the experimental results can be understood within our model, which assumes an ideal 2D ring weakly coupled to the emitter and the collector. There is a broad peak at $B \approx 0.07$ T in the smooth background of curve (a) in Fig. 2 of Ref. 3, which does not appear in our results. The exact reason for this peak is not clear. It may be due to the magnetic-field dependence of the coupling between the ring states and the two reservoirs, which is ignored in our calculation. As the magnetic field increases, the couplings between the two kinds of ring states (i.e., clockwise and counterclockwise) and the states in the reservoirs will change in the opposite directions. This could lead to structures in the mean magnetoresistance.

To reproduce all the details of the experimental results, such as the mean magnetoresistance and the oscillation amplitudes, a more sophisticated theory is needed, in which the detailed elastic scattering process at the connections between the ring and the two leads, and the inelastic scattering process in the ring, should be taken into account. However, what we have presented here has not only identified the main physics involved but also illustrated the importance of an analytic model that can be applied to many systems. Further details and applications of the model will be published elsewhere.²²

We would like to thank M. Boero and J. Matthias for helpful discussions. This work was partly funded by the UK EPSRC and ESPRIT Research Action No. 6536.

¹C. P. Umbach, S. Washburn, R. B. Laibowitz, and R. A. Webb, *Phys. Rev. B* **30**, 4048 (1984).
²V. Chandrasekhar, M. J. Rooks, S. Wind, and D. E. Prober, *Phys. Rev. Lett.* **55**, 1610 (1985).
³J. Liu, W. X. Gao, K. Ismail, K. Y. Lee, J. M. Hong, and S. Washburn, *Phys. Rev. B* **48**, 15 148 (1993).
⁴G. Timp *et al.*, *Phys. Rev. Lett.* **58**, 2814 (1987); C. J. B. Ford *et al.*, *J. Phys. C* **21**, L325 (1988); A. M. Chang and T. Y. Chang, *Bull. Am. Phys. Soc.* **38**, 229 (1993); J. B. Pieper and J. C. Price, *Phys. Rev. Lett.* **72**, 3586 (1994).
⁵Y. Gefen, Y. Imry, and M. Ya. Azbel, *Phys. Rev. Lett.* **52**, 129 (1984); M. Büttiker, Y. Imry, and M. Ya. Azbel, *Phys. Rev. B* **30**, 1982 (1984).
⁶M. Büttiker, Y. Imry, R. Landauer, and S. Pinhas, *Phys. Rev. B* **31**, 6207 (1985).
⁷J. K. Jain, *Phys. Rev. Lett.* **60**, 2074 (1988).
⁸G. W. J. Beenakker, H. van Houten, and A. A. M. Staring, *Phys. Rev. B* **44**, 1657 (1991).
⁹C. J. B. Ford *et al.*, *Phys. Rev. B* **49**, 17 456 (1994).
¹⁰P. A. Lee and A. D. Stone, *Phys. Rev. Lett.* **55**, 1622 (1985).
¹¹M. Büttiker, Y. Imry, and R. Landauer, *Phys. Lett.* **96A**, 365 (1983).
¹²H. F. Chung, E. K. Riedel, and Y. Gefen, *Phys. Rev. Lett.* **62**, 587 (1989).

¹³A. Szafer and B. L. Altshuler, *Phys. Rev. Lett.* **70**, 587 (1993); M. V. Berry and J. P. Keating, *J. Phys. A* **27**, 6167 (1994).
¹⁴L. P. Levy *et al.*, *Phys. Rev. Lett.* **64**, 2074 (1990); V. Chandrasekhar *et al.*, *ibid.* **67**, 3587 (1991).
¹⁵D. Mailly, C. Chapelier, and A. Benoit, *Phys. Rev. Lett.* **70**, 2020 (1993).
¹⁶Y. Avishai, Y. Hatsugai, and M. Kohmoto, *Phys. Rev. B* **47**, 9501 (1993); T. Chakraborty and P. Pietilainen, *ibid.* **50**, 8460 (1994).
¹⁷G. Montambaux *et al.*, *Phys. Rev. B* **42**, 7647 (1990).
¹⁸G. Kirczenow, *Superlatt. Microstruct.* **14**, 237 (1994).
¹⁹A. Groshev, I. Z. Kostadinov, and I. Dobrianov, *Phys. Rev. B* **45**, 6279 (1992).
²⁰D. Eliyahu, R. Berkovits, M. Abraham, and Y. Avishai, *Phys. Rev. B* **49**, 14 448 (1994).
²¹B. I. Halperin, *Phys. Rev. B* **25**, 2185 (1982).
²²W. -C. Tan and J. C. Inkson (unpublished).
²³D. Yoshioka and H. Fukuyama, *J. Phys. Soc. Jpn.* **61**, 2368 (1992); B. L. Johnson and G. Kirczenow, *Phys. Rev. B* **47**, 10 563 (1993); P. Hawrylak, *Phys. Rev. Lett.* **71**, 3347 (1993).
²⁴W. -C. Tan, J. C. Inkson, and G. P. Srivastava, *Semicond. Sci. Technol.* **9**, 1305 (1994); K. -F. Berggren *et al.*, *Phys. Rev. Lett.* **57**, 1769 (1986).
²⁵M. Büttiker, *Tunneling in Semiconductors*, edited by L. L. Chang *et al.* (Plenum, New York, 1991), p. 213.